

Integrating Bayesian groundwater mixing modeling with on-site helium analysis to identify unknown water sources

Andrea L. Popp^{1,2}, Andreas Scheidegger³, Christian Moeck¹, Matthias S.
Brennwald¹, Rolf Kipfer^{1,2,4}

¹Department of Water Resources and Drinking Water, Eawag, Swiss Federal Institute of Aquatic Science
and Technology, 8600 Dübendorf, Switzerland

²Department of Environmental Systems Science, ETH Zurich, 8000 Zurich, Switzerland

³Department of Systems Analysis, Integrated Assessment and Modelling, Eawag, 8600 Dübendorf,
Switzerland

⁴Department of Earth Sciences, ETH Zurich, 8000 Zurich, Switzerland

This document is the accepted manuscript version of the following article:

Popp, A. L., Scheidegger, A., Moeck, C., Brennwald, M. S., & Kipfer, R. (2019). Integrating bayesian groundwater mixing modeling with on-site helium analysis to identify unknown water sources. *Water Resources Research*.
<https://doi.org/10.1029/2019WR025677>

Corresponding author: Andrea L. Popp, andrea.popp@eawag.ch

12 **Key Points:**

- 13 • On-site ^4He analysis reliably substitutes for expensive and time-consuming lab-
14 based ^4He analysis.
- 15 • We present a Bayesian groundwater mixing model explicitly considering un-
16 known end-members and tracer-related uncertainties.
- 17 • Unknown water sources can be identified by combining the Bayesian mixing
18 model and ^4He analyzed on-site.

Abstract

Analyzing groundwater mixing ratios is crucial for many groundwater management tasks such as assessing sources of groundwater recharge and flow paths. However, estimating groundwater mixing ratios is affected by various uncertainties, which are related to analytical and measurement errors of tracers, the selection of end-members and finding the most suitable set of tracers. Although these uncertainties are well recognized, it is still not common practice to account for them. We address this issue by using a new set of tracers in combination with a Bayesian modeling approach, which explicitly considers the possibility of unknown end-members while fully accounting for tracer uncertainties. We apply the Bayesian model we developed to a tracer set which includes helium (^4He) analyzed on-site to determine mixing ratios in groundwater. Thereby, we identify an unknown end-member, that contributes up to $84\pm 9\%$ to the water mixture observed at our study site. For the ^4He analysis, we use a newly developed Gas Equilibrium Membrane Inlet Mass Spectrometer (GE-MIMS), operated in the field. To test the reliability of on-site ^4He analysis, we compare results obtained with the GE-MIMS to the conventional lab-based method, which is comparatively expensive and labor intensive. Our work demonstrates that (i) tracer-aided Bayesian mixing modeling can detect unknown water sources, thereby revealing valuable insights into the conceptual understanding of the groundwater system studied and ii) on-site ^4He analysis with the GE-MIMS system is an accurate and reliable alternative to the lab-based analysis.

1 Introduction

A groundwater sample usually consists of a mixture of water sources with different renewal rates such as fossil groundwater, decadal-age groundwater or recently infiltrated river water (e.g., Turnadge & Smerdon, 2014). The degree of mixing mostly depends on the aquifer’s heterogeneity and the extent of the well screen (e.g., Jasechko, 2016). Quantifying mixing ratios is key for assessing groundwater recharge (e.g., Beyerle et al., 1999) and groundwater vulnerability to pollution (e.g., Jasechko, 2016), and is thus essential to manage water resources sustainably (Pelizardi et al., 2017).

Groundwater mixing models rely on known concentrations of conservative tracers to quantify the fractions of different water sources contributing to a water sample (e.g., Carrera et al., 2004; Barthold et al., 2011; Cook & Dogramaci, 2019). Mixing ratios are estimated by comparing tracer concentrations in the sampled mixture with the concentrations of previously determined end-members (i.e., signatures of different water sources) by means of a mass balance approach (e.g., Christophersen et al., 1990; Hooper et al., 1990; Sanborn et al., 2016). In a bivariate tracer-tracer plot, end-members represent the most extreme values, with the sampled mixtures lying in between the end-member data points (Fig. S1 in the Supporting Information).

The first step to estimate groundwater mixing ratios is to determine end-members. This is mostly a conceptual step based on a sound understanding of the respective groundwater system e.g., through previous research or water table heads (e.g., Rueedi et al., 2005). It can, however, be aided by methods based on Principal Component Analysis (PCA), which find the minimum number of end-members to sufficiently explain the observed variability of a given tracer set (Christophersen & Hooper, 1992; Valder et al., 2012; Pelizardi et al., 2017). The second step consists of calculating the mixing ratios for the identified end-members based on the tracer concentrations of each sample using a mass-balance approach (in which by definition the fractions of each end-member for a mixed sample have to add up to 1).

Previous research has demonstrated that estimated mixing ratios derived from different tracers are not necessarily consistent (e.g., Carrera et al., 2004)—an issue which is usually handled by employing a least-squares approach to find the best fit of estimated mixing ratios (e.g., Christophersen et al., 1990). It has also been shown that tracer set size and composition as well as the correct identification of end-members have a substantial influence on the derived mixing ratios and that, in general, larger tracer sets yield more robust estimates (Barthold et al., 2011; Delsman et al., 2013).

Such discrepancies stem not only from uncertainties related to inconsistencies in sampling and measurement procedures (i.e., during field work and with regard to analytical measurement precision), but also from the underlying assumptions regarding conventional end-member mixing itself. These assumptions include that: (i) a water sample can be explained as a linear mixture of end-members (e.g., Delsman et al., 2013), (ii) the tracers behave conservatively, at least in the sense that any chemical reaction is much slower than the mixing process itself (e.g., Valder et al., 2012), (iii) tracer signals of each species are sufficiently distinct (e.g., Pelizardi et al., 2017), (iv) the chemical signatures of end-members are constant over time (e.g., Hooper et al., 1990), and (v) all end-members are identified correctly (Carrera et al., 2004; Delsman et al., 2013). These assumptions must either be justified or systematic uncertainties must be accounted for (in addition to tracer-related uncertainties). Although it is widely acknowledged that mixing ratios are associated with high uncertainties (e.g., Hooper, 2003; Carrera et al., 2004; Rueedi et al., 2005; Delsman et al., 2013), few attempts have been made to account for them. Hooper et al. (1990) calculated the uncertainty of the mixing ratios based on linear approximation. Brewer et al. (2002) build a hierarchical Bayesian model that allows us to infer the tracer uncertainty of the end-member concentrations. The approach of Delsman et al. (2013) is similar, however, it is based on an informal likelihood function, which is constructed based to the measurement uncertainties. In contrast, Christophersen et al. (1990) and Hooper (2003) tested by means of a PCA if a data set could be at all explained by a mixing

model (without defining the end-members). This can be seen as a test of the fifth assumption. Neglecting systematic uncertainties related to the assumptions mentioned above leads to overconfident estimates of groundwater mixing ratios, which can result in false and unreliable conclusions. While assumptions (i)–(iv) can typically be well defended, assumption (v) is most critical.

Besides traditional end-member mixing models, different Bayesian approaches have evolved in isotope hydrology and geochemistry to constrain source contributions of various Earth surface processes (e.g., Soulsby et al., 2003; Erhardt & Bedrick, 2013; Arendt et al., 2015; Davis et al., 2015; Blake et al., 2018; Parnell & Inger, 2019).

We present a newly developed Bayesian groundwater mixing model that builds on existing Bayesian approaches by adding two new features to better represent and describe the aforementioned uncertainties: first, our model explicitly considers uncertainties originating from sampling and measuring of tracer species; second, the model accounts for the possibility of principally unknown end-members (from here on referred to as *residual end-member*). Not only can our approach express the resulting uncertainties of the estimated end-member mixing ratios, it also allows to quantify the mixing ratios of the residual end-member and its tracer concentrations. Separating these two error sources is important for the interpretation, as otherwise any model mismatch would be “explained” by poor measurements alone. While it is possible to reach similar conclusions by carefully interpreting residuals of traditional end-member mixing models (e.g., Hooper, 2003), more indirect reasoning is required to weight the observation errors accurately.

In addition to the development of the Bayesian mixing model, we introduce the use of ^4He analyzed on-site as a tracer to estimate groundwater mixing ratios. The inert biochemical nature of the noble gas helium (mainly ^4He) makes it an ideal tracer to study groundwater dynamics, e.g., such as recharge and surface water–groundwater interactions (e.g., Price et al., 2003; Marty et al., 1993; Kulongoski et al., 2008; Gardner

et al., 2011; Müller et al., 2016; Batlle-Aguilar et al., 2017). Typically, conventional lab-based ^4He analysis is costly and labor-intensive, therefore, only a few specialized laboratories can carry out such analyses on a routine basis. Here, we use ^4He data analyzed in the field with a recently developed portable mass spectrometry system (Brennwald et al., 2016) to estimate mixing ratios. Moreover, to test and validate the suitability of the new system, we compare ^4He concentrations obtained in the field with concentrations analyzed at the noble gas laboratory of the Swiss Federal Institute of Technology in Zurich, Switzerland.

Our study aims (i) to derive a novel methodology for estimating groundwater mixing ratios by explicitly accounting for the potential presence of unknown end-members and tracer uncertainties and (ii) to assess the suitability of on-site ^4He analysis using a portable mass-spectrometry system by comparing it to conventional lab-based noble gas analysis.

2 Site Description and Conceptual Model

Our study site, the Hardwald, is located in north-western Switzerland in close proximity to the Rhine river and the city of Basel and covers about 10 km² of mainly urban and industrial areas (Fig. 1).

The conceptual hydrogeological model (based on previous research; Moeck et al., 2016; Moeck, Radny, Popp, et al., 2017) assumes two main aquifers at the site (Fig. 2): an unconfined Quaternary sand-gravel aquifer, which is overlying a karstified Upper Muschelkalk aquifer (Moeck et al., 2016). The former consists of unconsolidated, highly conductive ($k \sim 270$ m/d), fluvial Quaternary sediments (Spottke et al., 2005). The latter mainly consists of low-conductive limestone ($k \sim 10$ m/d), is fractured and partly confined (Spottke et al., 2005; Moeck et al., 2016). In both aquifers, groundwater generally flows from southeast to northwest in the direction of the Rhine River. Towards the Rhine, an impermeable boundary formed of limestone of the

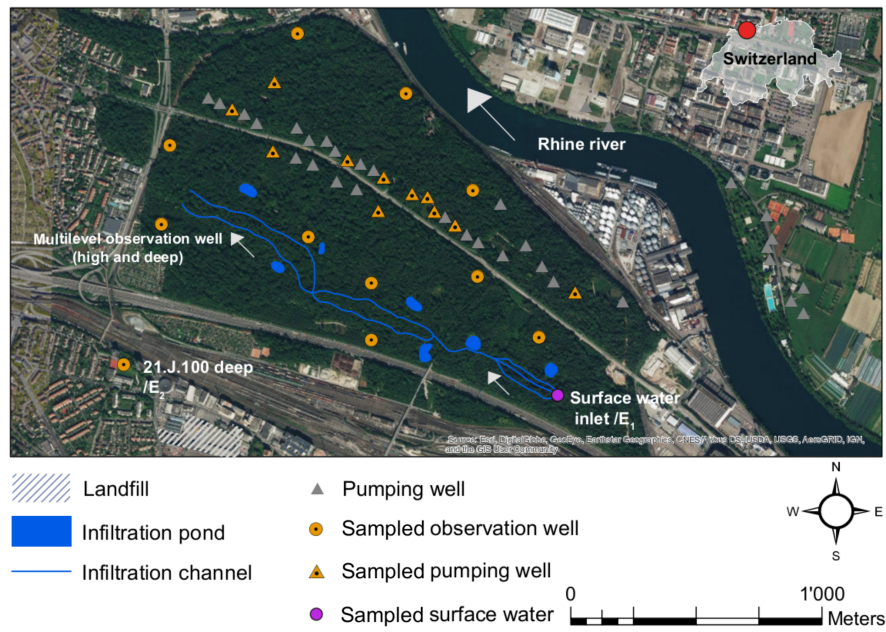


Figure 1. Study site showing the Hardwald with the infiltration system of channels and ponds (blue), and its surrounding area. Sampling points are marked as symbols containing black dots, the point in magenta indicates the inlet of Rhine water to the infiltration system.

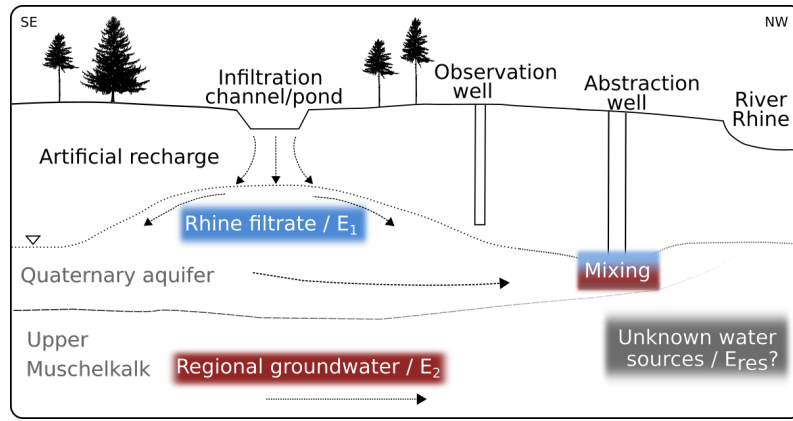


Figure 2. Conceptual model of the hydrogeological setting and flow system showing the local groundwater mound caused by the artificial infiltration, and the mixing between recently infiltrated Rhine water (i.e., end-member 1, E_1 in blue), regional groundwater (i.e., end-member 2, E_2 in red) and potential unknown water sources (i.e., residual end-member, E_{res} in gray).

Middle Muschelkalk exists (Moeck et al., 2016). This boundary fosters up-welling of groundwater from the Upper Muschelkalk aquifer into the Quaternary sand-gravel aquifer towards the northern part of the study area (see Spottke et al., 2005 and Moeck et al., 2016 for more details). Moreover, groundwater mixing between both aquifers is most likely amplified by groundwater pumping (Moeck, Radny, Popp, et al., 2017). The Upper Rhine Graben—a highly deformed flexure zone—constitutes the western boundary of the study area (Moeck et al., 2019). There the complex hydrogeological features (i.e., fault zones and fractures) result in high uncertainties in the hydraulic conductivity distribution (Moeck et al., 2019; see Fig. S2 for a simplified illustration of the bedrock units mentioned above).

Since the 1950s, groundwater has been abstracted from a pumping well field (Fig. 1) within the Hardwald site to produce drinking water. In response to an increased water demand caused by a growing population and industry, managed aquifer recharge (MAR) was introduced in 1958 by taking raw water from the Rhine and divert-

ing it through channels and ponds (Figs. 1 and 2). From there the water naturally infiltrates into the underlying Quaternary aquifer with an average rate of 95 000 m³/day. As the artificial recharge exceeds the water withdrawal by a factor of two, a local groundwater mound forms at the recharge site (Fig. 2; Moeck, Affolter, et al., 2017). This groundwater mound serves as a natural barrier against water inflow from upstream areas by reversing the natural groundwater flow direction—a crucial feature to protect the drinking water production area as the upstream region is exposed to several potential sources of contamination (e.g., surrounding industry; Fig. 1).

Figure 2 also shows potential mixing pathways between the artificially infiltrated water (i.e., Rhine water, E_1), unknown end-members (E_{res}) and regional groundwater (E_2), which is known to contain certain contaminants (Moeck, Radny, Popp, et al., 2017). Traces of these contaminants can be found in the abstracted drinking water (Moeck et al., 2016). The admixture of undesirable regional groundwater to the abstracted drinking water is likely to occur given the hydrogeological setting and groundwater withdrawal. The fraction of regional groundwater admixed to the abstracted drinking water might differ, though, depending on the specific well location. Therefore, a spatially resolved, quantitative assessment of the admixture of regional groundwater in the abstracted water is key for the future management of this MAR site, which provides drinking water for more than 200 000 people living in the agglomeration of Basel.

3 Material and Methods

To determine groundwater mixing ratios, we analyzed a set of environmental tracers. From August 15th to August 25th in 2016, we sampled 20 groundwater observation and pumping wells all over the study area as well as the infiltration channel from which the Rhine water is being distributed (Fig. 1). On December 5th 2017, we sampled another three pumping wells within the study area for the same parameters.

For sampling, we either used already pre-installed pumps at the pumping wells or a submersible pump (MP1, Grundfos) for the observation wells. We started sampling after purging all wells three times according to their volume and after field parameters (O_2 , EC, temperature, pH) had reached a stable level (i.e., at least three consecutive measurements with same concentrations within analytical uncertainty; analyzed with a calibrated HACH HQ40D portable multi meter). Details for the sampling procedure for the individual tracers are given below and in the Supporting Information. All tracer data, well locations and well depths are available in the Supporting Information (Dataset S1).

During our sampling campaigns, the MAR system was operated under standard conditions (i.e., average water infiltration and abstraction rates which govern the hydraulic head distribution). Thus, hydraulic conditions representative for the standard operation of the MAR site were guaranteed.

3.1 Hydro-Chemical Parameters

Rock-water interactions lead to an increase in hydro-chemical species (Ca^{2+} , Mg^{2+} , Na^+ , K^+ , Cl^- , H_4SiO_4 , SO_4^{2-} , EC, alkalinity, total hardness and pH) in groundwater with respect to precipitation, which leave characteristic chemical fingerprints (Piper, 1944; Cook & Herczeg, 2000). These fingerprints render such hydro-chemical species suitable to identify water flow paths and mixing of waters of different origin (e.g., Currell & Cartwright, 2011; Dogramaci et al., 2012; Skrzypek et al., 2013). We acknowledge that the parameters EC, pH, alkalinity and total hardness are correlated with the concentrations of dissolved ions present in a solution. They were, however, analyzed independently (see Table S2), and are thus accounted for as individual tracers.

We collected samples to analyze all hydro-chemical parameters as unfiltered water samples in one liter Schott glass flasks. The flasks were immediately cooled after

sampling and analyzed the following day at Eawag (for methods, limits of quantification and analytical errors please see Table S2).

3.2 Analysis of ^4He

Helium is a noble gas, which has often been used to quantify groundwater residence times and aquifer recharge (e.g., Kulongoski et al., 2008; Gardner et al., 2011; Müller et al., 2016; Batlle-Aguilar et al., 2017). ^4He is slowly produced by α decay of ^{238}U , ^{235}U and ^{232}Th in the rock matrix and continuously accumulates in groundwater, which makes it an excellent indicator of long groundwater residence times, in the order of several hundreds to thousands of years, depending upon aquifer material and geology (e.g., Gardner et al., 2011). Please see Texts S2.1 and S2.2 of the Supporting Information for a description about the on-site and lab-based ^4He analyses.

3.3 Selection of End-Members

The commonly used end-member mixing analysis—EMMA—was first presented for estimating mixing ratios in stream waters (Christophersen et al., 1990) and is still mainly applied in surface water studies (e.g., Hooper, 2003; Bernal et al., 2006; Barthold et al., 2011; Valder et al., 2012). EMMA often involves PCA to elucidate the minimum number of end-members of a water sample. However, PCA is not appropriate for a small number of samples, which is often the case for groundwater studies.

In groundwater samples, the identification and selection of potential end-members is commonly better constrained than in surface waters due to the dampening effect of temporal tracer variations within an aquifer (Carrera et al., 2004). Thus, tracer concentrations in groundwater systems show less temporal variability compared to tracer concentrations in surface waters. We therefore argue that for estimating mixing ratios in groundwater, identifying potential end-members based on expert knowledge such as a conceptual model (e.g., pre-existing data or previous studies) and by screening through bivariate tracer-tracer plots is a valid and robust approach.

Consequently, we selected end-members according to our conceptual model of the field site, which is based on previous research conducted in this area (Spottke et al., 2005; Moeck et al., 2016; Moeck, Radny, Popp, et al., 2017). Our selected end-members generally confirmed our conceptual model by representing the most extreme values in bivariate tracer-tracer distribution for most tracers used in this study (Fig. S1). We thereby identified two end-members: end-member E_1 , which represents the infiltrated Rhine water (sample taken from the channel from which the Rhine water is distributed), and end-member E_2 , which represents regional groundwater being sampled from observation well *21.J.100-deep* (Fig. 1). This well is located in the southwestern area of the study site, which is hardly affected by the artificial infiltration and is therefore representative for the regional groundwater component (Fig. 2).

Although most samples fall well within the linear mixing lines of the two predefined end-members (Fig. S1), we principally cannot exclude the presence of an unknown water source. In cases where the data are not well reproduced by binary mixing of the two end-members considering tracer uncertainties, our model assigns a residual end-member component (E_{res}) to explain the observed tracer concentrations (see next section for a comprehensive description).

3.4 Bayesian Mixing Model

Conventional end-member mixing models (e.g., Christophersen et al., 1990) estimate the concentration $C[t]$ of a tracer substance t at a given well as a mixture of M pre-selected end-members E_m , with corresponding concentrations $C_{E_m}[t]$:

$$C[t] = r_1 C_{E_1}[t] + \dots + r_M C_{E_M}[t] + \epsilon_t, \quad t = 1 \dots T \quad (1)$$

where r_m , $m = 1 \dots M$ are non-negative mixing ratios that sum up to one, and T is the number of tracer substances. The mixing ratios are usually estimated by minimizing the errors ϵ_t with a non-negative least-squares approach. We emphasize that this

error term allows no direct interpretation because it lumps together all sources of uncertainties.

To achieve an explicit handling of uncertainties, we extend the classical model (Equation 1) by first incorporating observational errors due to tracer-related uncertainties, and by second accounting for systematic biases due to potentially unobserved end-members.

3.4.1 Observation Errors

All measured tracer concentrations are subject to errors. The characteristics for these errors for any tracer species can be described by means of an *observation model*, $p(C^{\text{obs}} | C)$, which is the conditional probability distribution of the observed but erroneous concentrations C^{obs} if one knew the true observation C . Such distributions are either derived from repeated measurements or expert knowledge (i.e., a realistic estimation of the overall tracer uncertainty of a sample). For this study we defined the observation model as

$$p(C^{\text{obs}} | C) = N(C, \rho C)$$

i.e., a normal distribution with a standard deviation of ρ times the mean. This is a very simplistic choice. However, other—potentially non-Gaussian—observation models can readily be used instead.

With the help of the observation model the “true” but unknown concentrations C are inferred from the tracer data. To achieve this, the true concentrations C are treated as additional model parameter, similar to the Bayesian total error analysis approach from surface hydrology (Kavetski et al., 2006). The observation model is part of the likelihood function and accounts for all tracer-related uncertainties. The advantage of this approach is that for the rest of the model derivation we can pretend to know the true, error-free concentration C .

In our case, we assume an overall tracer uncertainty of $\rho = 10\%$ for each individual tracer concentration based on an analytical error of 1-5% (depending on the tracer species) plus uncertainties due to inconsistencies in the sampling and analytical procedure. For end-member E_1 (Rhine water) we assume an overall tracer uncertainty of 20% due to the higher variability of tracer concentrations in surface water relative to groundwater. This assumption is corroborated by the variance of time series data of hydro-chemical tracers (i.e., major ions, pH, EC, total hardness, alkalinity) observed at the Rhine monitoring station (located about 7 km downstream of our study area): time series data that most likely represent the time frame of infiltration (i.e., the last 3 months before our sampling took place) show a mean variance of tracer concentrations between 10% and 15% (in 2016 and 2017, respectively).

3.4.2 *Residual End-Member*

As described above, total tracer-related uncertainties are 10% (20% for E_1 , respectively) accounting for sampling and measurements errors. Even if tracer concentrations were error free, we would not expect the classical model to perfectly match our observations due to the systematic bias of not accounting for all end-members present in a system.

To avoid this strong assumption of perfect end-member identification, we introduce a hypothetical *residual* end-member (E_{res}). One can easily imagine that a number of unknown end-members actually exist in any complex environmental system. Therefore, we extend the mixing model (1) with a residual end-member:

$$C[t] = r_1 C_{E_1}[t] + \dots + r_M C_{E_M}[t] + r_{M+1} C_{E_{\text{res}}}[t], \quad t = 1 \dots T \quad (2)$$

As the concentrations $C_{E_{\text{res}}}[t]$ of the unknown end-member cannot be observed, they are treated as additional model parameters. This approach has the advantage that not only the fraction r_{M+1} is acquired but also the concentration profile of E_{res} is revealed, which might allow to identify the hydrogeological origin of E_{res} .

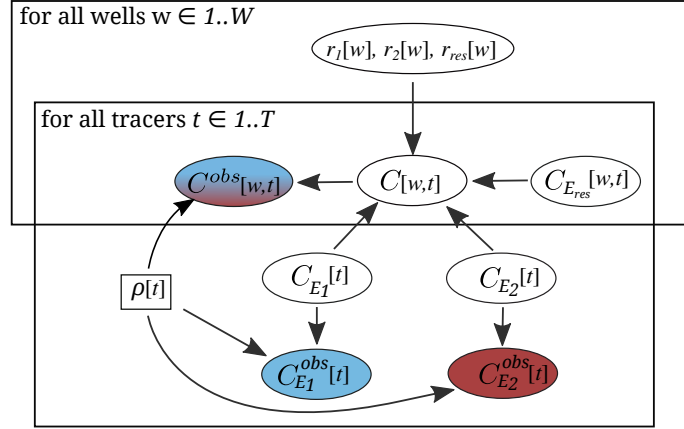


Figure 3. Graphical representation of the probabilistic mixing model for two end-members (E_1 and E_2). Round nodes represent random variables, the square node a constant value, and the boxes repetition over the index. The colored nodes are observations on which the other random variables are conditioned on.

It is important to notice that Equation 2 only makes use of the true (inferred) concentrations so that the residual end-member corrects for systematic deviations that cannot be explained by tracer-related uncertainties.

3.4.3 Parameter Inference

The introduction of the observation model and the residual end-member considerably increase the number of parameters to estimate, so that in a frequentist setting (e.g., with maximum likelihood estimation) no unique best parameter values can be determined. However, well defined parameter distributions can still be inferred with Bayesian inference by using weak and intuitive prior distributions.

Figure 3 provides a conceptual overview of the dependency of the involved quantities: all round nodes represent random variables whose distribution are defined by the model according to the values of the incoming nodes. For the colored nodes observa-

tions are available on which all the other nodes are conditioned (i.e., inferred) on. The boxes denote repetitions over the index. For example different “true” concentrations of the two end-members are estimated for each tracer. A separate concentration of the residual end-member is inferred for every tracer and well. The complete mathematical derivation of the corresponding likelihood function used for Bayesian inference can be found in the Supporting Information Text S2.

Additional prior distributions are required for the inference of the unknown quantities. We define the following prior distributions: (i) a non-informative, flat prior $U(0, \infty)$ for the true end-member concentrations, (ii) a Dirichlet($1, \dots, 1$) distribution for the mixing ratios, which defines an uninformative distribution over a simplex that guarantees $\sum_{m=1}^{M+1} r_m = 1$ and $0 \leq r_m$, $m = 1, \dots, M + 1$ (see Delsman et al., 2013), and (iii) an informative prior for the residual end-member concentrations. For the latter, we selected uniform distributions with the lower and upper limits being $\pm 20\%$ of any observed tracer concentration.

3.4.4 Implementation

The model was implemented in STAN (Carpenter et al., 2017)—a probabilistic programming language well suited for Bayesian inference. We generated three independent Monte Carlo Markov Chains (Kruschke, 2015) with a length of 15 000, discarding the first 5 000 samples as burn-in. We pre-processed and visualized all data using R (R Core Team, 2018).

4 Results

4.1 Comparison between On-Site and Laboratory-Based ^4He Analysis

Due to the time demanded for the lab-based ^4He analysis, we limited the analysis of copper tube samples to a subset ($n=17$) of the 23 wells analyzed in this study. With the GE-MIMS system, however, we analyzed ^4He at all 23 wells. We compared the

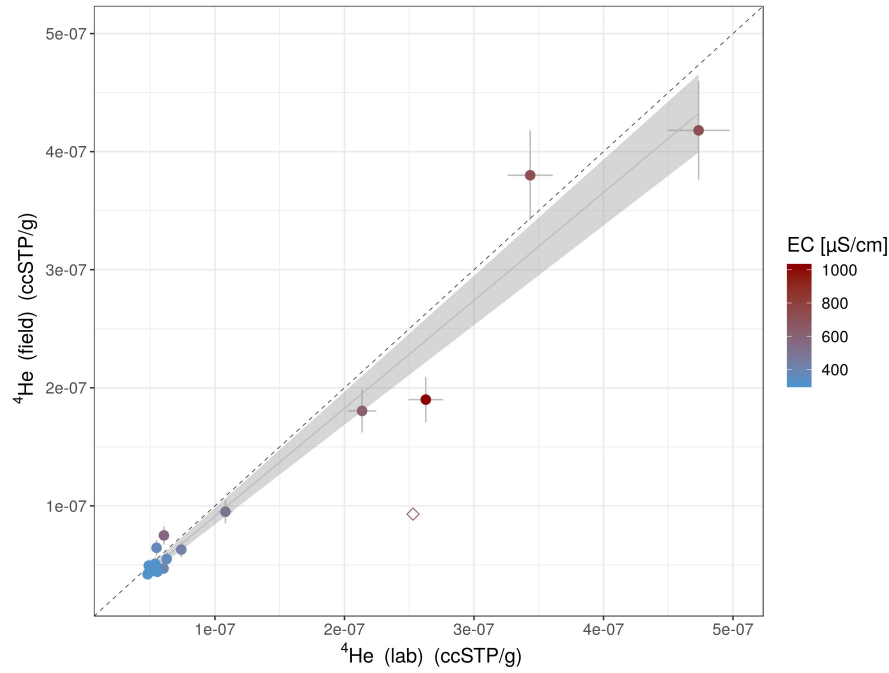


Figure 4. Comparison between lab-based and on-site analysis of ^4He concentrations. The gray band shows the 95% confidence interval of a linear regression (neglecting one outlier marked as a diamond); error bars represent analytical measurement uncertainties. The data indicate, that ^4He and EC concentrations increase simultaneously, suggesting higher mineralization with increasing residence time.

two methods to test whether the GE-MIMS system can reliably substitute the lab-based ^4He analysis. The high linear correlation (adjusted $R^2=0.98$, $\text{RMSE}=2.4 \times 10^{-8}$, $p < 0.001$; $n=16$ after neglecting one outlier, with outlier adjusted $R^2=0.94$, $p < 0.001$) between the ^4He analyses demonstrates that the GE-MIMS is well suited for high precision ^4He analysis under field conditions (Fig. 4; data are available in Table S1). Overall, these results show that the two methods yield similar concentrations, which consequently allows for the use of on-site analyzed ^4He concentrations as tracer to estimate groundwater mixing ratios.

4.2 Model Sensitivity Analysis using Different Tracer Sets

Theoretically, any set of conservative tracers to calculate mixing ratios can be used. Given the various tracers obtained by us, we explore the effect of different—in number and composition—sets of tracers to test their influence on the estimated mixing ratios. In particular the contribution (r_{M+1}) of the residual end-member (E_{res}) is of fundamental interest, because it can be interpreted as a measure of how internally consistent a tracer set is with regard to the assumed binary mixing hypothesis.

Table 1 specifies all the different tracer set sizes and compositions we assessed. The tracer sets differ from “easy to measure” tracers (i.e., feasible to obtain data with a hand-held probe) such as pH and EC (tracer set 1: *TS1*), to more advanced sets consisting of standard hydro-chemical tracers such as major ions, alkalinity and total hardness (*TS2–TS4*).

We also tested one tracer set (*TS5*) that includes all tracers obtained including ^4He but also less conservative species (i.e., nitrate and sulfate), which are sometimes used to calculate mixing ratios (e.g., Soulsby et al., 2003; Delsman et al., 2013; Moeck, Radny, Auckenthaler, et al., 2017). *TS6* consists only of ^4He concentrations determined in the field. Finally, *TS7* includes all tracers except for nitrate and sulfate.

The results of this sensitivity analysis using different tracer sets demonstrate that model uncertainties (i.e., amount of E_{res}) vary depending on the tracer set used (Fig. 5). These findings indicate that, in general, uncertainty tends to decrease with increasing numbers of tracers. This is, however, only true as long as the tracers are consistent, which is not the case for *TS5*.

The simplest tracer set (*TS1*) has, with about 20%, the highest average contribution of E_{res} . Using more than two tracers (e.g., *TS2*) or adding more tracers to *TS1* (*TS3–4*) considerably decreases the model uncertainty. *TS5* reveals that including the less conservative species nitrate and sulfate results in higher model uncertainties.

Table 1. Mixing model sensitivity analysis by testing different tracers sets. The mean estimated ratio of an unknown end-member (E_{res}) indicates the goodness of fit of the mixing model depending on the respective tracer set.

Tracer Set	Used Tracers	Number of Tracers
<i>TS1</i>	pH, EC	2
<i>TS2</i>	hydro-chemical species (Ca^{2+} , Mg^{2+} , Na^+ , K^+ , Cl^- , H_4SiO_4)	6
<i>TS3</i>	pH, EC, hydro-chemical species	8
<i>TS4</i>	pH, EC, hydro-chemical species, alkalinity, total hardness	10
<i>TS5</i>	pH, EC, hydro-chemical species, alkalinity, total hardness, nitrate, sulfate, ^4He	13
<i>TS6</i>	^4He	1
<i>TS7</i>	pH, EC, hydro-chemical species, alkalinity, total hardness, ^4He	11

Only using ^4He concentrations as a single tracer (*TS6*) shows that despite a low variability in E_{res} , the mean fraction of E_{res} is higher than in *TS2-4*. Overall, *TS7* yields the most robust results: it can explain most data by binary mixing of E_1 and E_2 and allocates higher fractions of an unknown end-member (31 ± 8 – $84 \pm 9\%$) only to four wells (Fig. 5). Consequently, we used *TS7* to estimate the mixing ratios given its apparent robustness compared to other tracer sets.

When comparing *TS4* (no ^4He) and *TS7* (*TS4* + ^4He), one could argue that both yield similarly acceptable results and that *TS4* is a reasonable approximation to estimate mixing ratios. However, when looking at specific wells (e.g., *21.C.206*, first column in Fig. 6), we note that including ^4He concentrations actually results in a considerably higher fraction of E_{res} . For the other two wells illustrated in Figure 6, adding ^4He concentrations only has a marginal effect. Figure 6 also clearly indicates that even though wells *21.A.17* and *21.A.18* are located adjacent to each other, their respective mixing ratios differ. Please see Figures S5 to S7 for the ternary diagrams showing mixing ratios of all wells for tracer sets 1, 4 and 7.

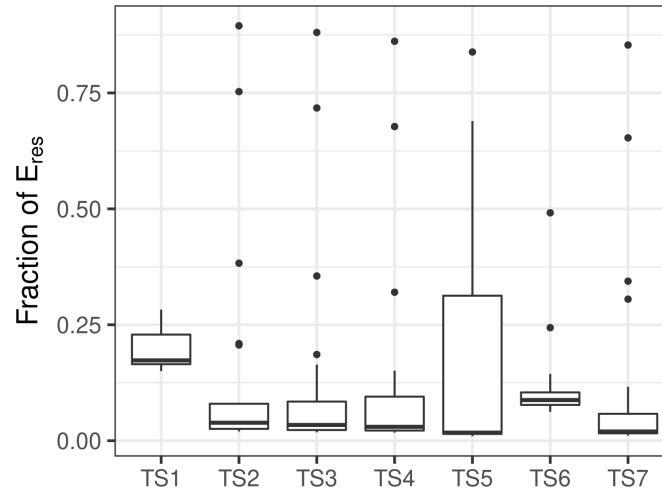


Figure 5. Sensitivity test of different sets of tracers shown in box plots: lower fractions of E_{res} indicate a better explanation of the available data with two end-members (i.e., E_1 and E_2) only (see Table 1 for information on the tracer sets and Fig. S4 for labels on all data points).

4.3 Estimated Mixing Ratios and their Uncertainties

Figure 7 illustrates the spatial distribution of estimated fractions of end-members (E_1 , E_2 and E_{res}) based on $TS7$. As expected, most wells in proximity to the infiltration area show a large fraction of recently infiltrated Rhine water (E_1 , e.g., up to $97\pm1\%$ at $21.C.215$; Fig. 7). Further away from the artificial recharge area, e.g., at pumping well $21.A.16$, the fraction of Rhine filtrate slightly decreases to $94\pm2\%$. Interestingly, the close-by pumping well $21.A.17$ shows with $88\pm4\%$ a comparatively low fraction of recently infiltrated water.

Towards the western border of the study area, which is (according to previous studies, Moeck et al., 2016; Moeck, Radny, Popp, et al., 2017) less impacted by the artificial recharge, the fraction of Rhine filtrate further decreases (e.g., $21.A.7$ with $70\pm4\%$ or $21.A.33$ with $85\pm3\%$ of E_1). Observation well $21.C.206$ —located at the western border of the study area—shows with $27\pm7\%$ an exceptionally low fraction of E_1 (compared to surrounding wells like $21.A.4$ with $89\pm2\%$) but simultaneously

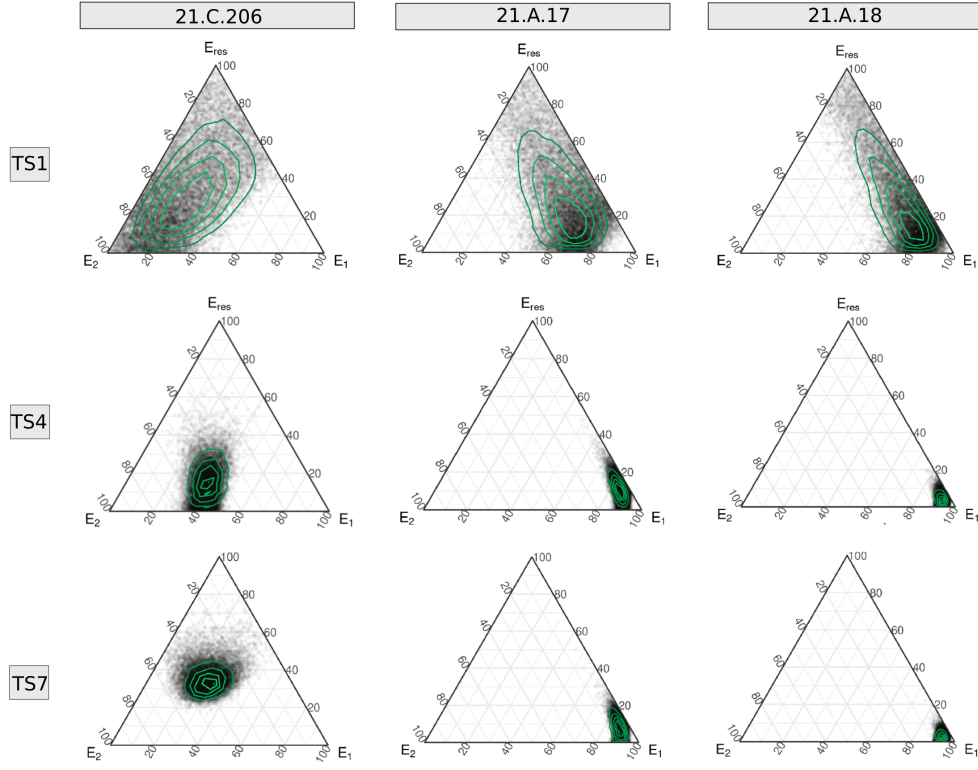


Figure 6. Ternary diagrams of the mixing ratios (%) of three different wells (*21.C.206*, *21.A.17*, *21.A.18*) for *TS1*, *TS4* and *TS7*, (representing tracer sets with increasing complexity, see Table 1). The assessment shows that with increasing tracer set size (from *TS1* to *TS4* to *TS7*) model uncertainty is reduced. Green contour lines show the probability density representing the estimated uncertainty.

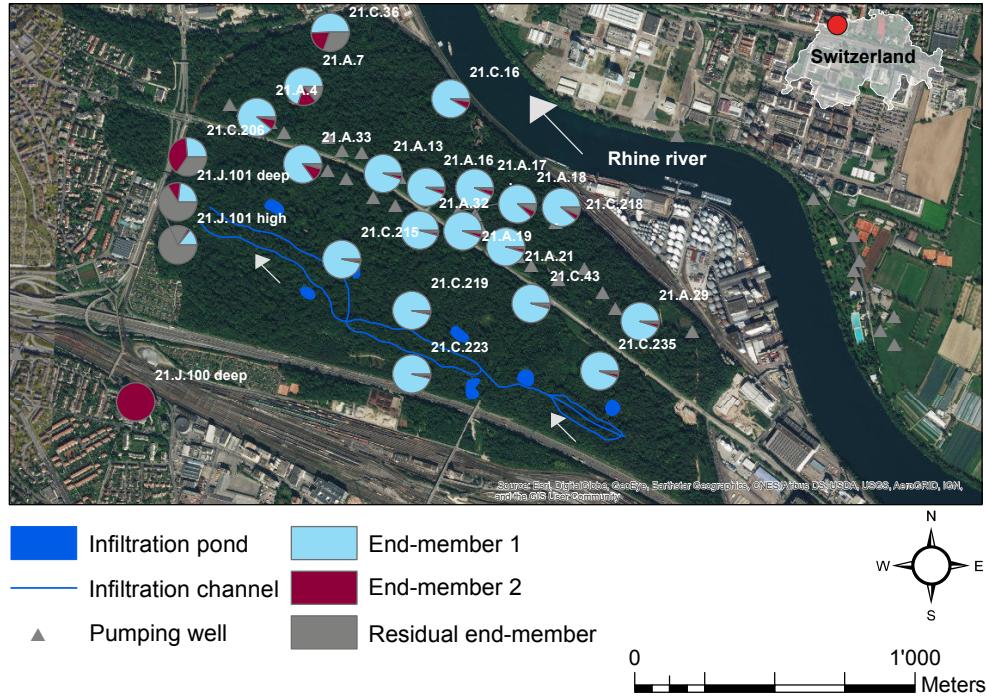


Figure 7. Spatial distribution of estimated mixing ratios. Blue represents end-member E_1 , red end-member E_2 , and grey stands for the residual end-member E_{res} , i.e. an unknown water source.

also has a relatively high fraction ($36 \pm 7\%$) of an unknown end-member (E_{res}). The by far highest fractions of E_{res} were detected in wells *21.J.101-high* ($84 \pm 9\%$) and *21.J.101-deep* ($66 \pm 12\%$). The mixing model attributed higher fractions of E_{res} only to one other well (*21.C.36* with $31 \pm 8\%$). All wells with a considerable fraction of E_{res} are being located at the western border of the study area.

Apart from these wells, three other wells (*21.A.17*, *21.A.7*, *21.C.218*) show moderate contributions ($6 \pm 5\%$ – $12 \pm 8\%$) of an unknown water source. The remaining wells exhibit only small fractions of E_{res} ($\leq 4 \pm 4\%$). All estimated mixing ratios and their uncertainties are illustrated in Figure S3 (based on Dataset S2). Overall, for most tracer species model-based estimates of tracer concentrations are in good agreement with the measured concentrations (see Fig. S8).

5 Discussion

5.1 Substituting Lab-Based with On-Site ^4He Analysis

The two methods compared for analyzing ^4He differ regarding sampling volume and technique, analytical procedure, calibration and data processing. Thus, the assumption that both methods yield in fact comparable results for ^4He concentrations is not straightforward.

Nonetheless, the statistically significant correlation between the two ^4He concentration data sets demonstrates that the results of the simple GE-MIMS system are as satisfying as those of the highly sophisticated lab-based method. Thus, these findings validate the accuracy and suitability of ^4He analysis using the GE-MIMS system and confirm that on-site methods can reliably substitute for conventional lab-based ^4He analysis, which is comparatively time demanding and labor intensive.

Moreover, we would like to highlight that during field work the portable MS guided the selection of the most interesting wells in quasi real-time, which allowed for very efficient sampling of an access restricted area.

5.2 Tracer Set Selection, Validity of Mixing Model and Study Limitations

We assessed the sensitivity of the mixing model outcome by testing different tracer sets. This approach shows that the most consistent results (i.e., most data can be explained by our selected end-members E_1 and E_2) are obtained by applying all analyzed tracers (including ^4He), except for the less conservative ones (nitrate and sulfate). These results highlight once more that using a combination of multiple, diverse tracers with different geochemical behavior is the most robust approach to quantify water mixing (e.g., Abbott et al., 2016; Tetzlaff et al., 2015). Thus, using a combination of geochemically different tracers is crucial to evaluate whether a mixing model yields meaningful and robust results. Furthermore, our findings show that less

conservative tracers should strictly be avoided when calculating mixing ratios because their use tends to increase mixing model uncertainties.

The ability of our mixing model to estimate the contribution of unknown residual end-members (E_{res}) and to account for tracer uncertainty separately turned out to be valuable. We acknowledge, however, that the implementation of such a Bayesian model also requires more assumptions to be pre-described explicitly. For example, uncertainties for each individual tracer analyzed at each individual well have to be determined and a prior distribution for the concentrations of the residual end-members must be defined. We explicitly state that these assumptions are to some degree subjective. However, they increase transparency and avoid over-interpretation of the results, and allow to test different assumptions. For instance, in our study, the concentrations of the residual end-members were not fixed across the wells allowing for the mixing model to estimate E_{res} and its geochemical composition for each well independently. We chose this approach because we had no expectation regarding the number of unobserved end-members present in our system.

By ascribing an overall tracer concentration uncertainty of 10% (and 20% for the infiltration water), we believe to conservatively account for all associated uncertainties including systematic biases, from sampling in the field to the final concentrations. A limitation of this study is that due to access restrictions to the drinking water protection site, we sampled the tracers only once. Thus, we have to assume that the temporal variability of tracer concentrations is neglectable or accounted for within the ascribed uncertainties. Since the attributed overall uncertainties are rather conservative, the estimated fractions of E_{res} also represent rather conservative estimates of unknown water sources present in our system. Moreover, we argue that the sampled tracer concentrations are representative as the site is artificially controlled by managed aquifer recharge and was sampled under standard operating conditions. To entirely rule out

the possibility of time variable end-members, one would need to acquire time series data of the groundwater end-members, which is beyond the scope of this study.

5.3 Adjustment of the Conceptual Model

In principle, our results are in line with previous studies conducted at the study site. By means of a cluster analysis, Moeck et al. (2016) identified observation well *21.C.206* to have a distinct geochemical signature that could not be classified with any other investigated well. Likewise, our assessment shows that *21.C.206* has an exceptional geochemical signature compared to most other wells (see Figs. 6 and 7). However, we can now explain these different geochemical characteristics by the presence of a high ratio ($36\pm 7\%$) of a previously unknown water source.

Moreover, pumping well *21.A.17* was found to exhibit a different hydrogeochemistry and higher micro-pollutant concentrations compared to most other wells in its vicinity and to be hydraulically connected to the underlying aquifer (Moeck et al., 2016; Moeck, Radny, Popp, et al., 2017). According to our analysis, these differences might originate from a higher fraction of regional groundwater (E_2) ($6\pm 2\%$) relative to the surrounding wells *21.A.16* and *21.A.18* (both $4\pm 2\%$).

Although Moeck, Radny, Auckenthaler, et al. (2017) report similar mixing ratios (based on the same selected end-members) compared to our study, they neglect the possibility of unknown end-members, which results in high standard deviations (more than 35%) in their estimated mixing ratios.

Thus, we demonstrate that the existing conceptual model of binary mixing of two water sources (i.e., E_1 and E_2) is not valid for the entire system. These findings require an adjustment of the conceptual model by acknowledging the contribution of unknown water sources (E_{res}), which were previously neglected.

Since E_{res} fractions are highest in the west (Fig. 7), we hypothesize that water of unknown origin occurs in the Hardwald site at its western boundary. The local

presence of E_{res} can therefore be interpreted as a third end-member and not as various different unknown water sources. As the Rhine Graben forms the western boundary of the study area (Fig. S2), it becomes apparent that E_{res} reflects water from this flexure zone, which provides a pathway for groundwater of deeper strata to ascend (Fig. 2). This conclusion is further reinforced since deep groundwater is expected to be high in helium (e.g., Stute et al., 1992). Wells (i.e., 21.C.36, 21.A.7, 21.C.206, 21.J.101.h, 21.J.101.d, 21.A.7, 21.C.36, 21.C.206; see Dataset S1) located at the western edge of the study area show indeed elevated ^4He concentrations.

In conclusion, water mixing through the flexure zone might be of greater importance for the water management of the Hardwald site than previously assumed. Consequently, water mixing at the study site can only be explained by at least three groundwater components and not by two as previously assumed.

6 Conclusions

According to Tetzlaff et al. (2015), there is an urgent need for a “more economic analysis of large sample numbers in conjunction with novel, tracer-aided modeling approaches” to improve our understanding of hydrological processes. By demonstrating the suitability of the portable GE-MIMS system as a substitute for the conventional lab-based analysis of ^4He (Fig. 4), we are able to introduce a new, more efficient method for dissolved (noble) gas analysis. Beyond proving the suitability of on-site ^4He analysis, our study shows that ^4He is as an excellent tracer to estimate groundwater mixing ratios and can help to reduce model uncertainty and to identify unknown water sources, e.g., water mixing through fault zones (Figs. 5 and 6).

Moreover, our sensitivity analysis emphasizes that mixing model uncertainties decrease with increasing numbers of conservative tracers (Fig. 5). By combining the most robust tracer set (TS7) with a Bayesian modeling framework, we can identify the

presence of a previously unknown water source and thereby improve our conceptual understanding of our study site (Figs. 7 and S3).

7 Outlook

The compact size of the portable GE-MIMS system allows for efficient (noble) gas analyses at remote locations (e.g., northern catchments, high altitudes) with a high spatio-temporal resolution. Therefore, it has great potential for a widespread application in locations where tracer data resolution is usually scarce due to time and cost limitations as well as access restrictions.

Although, we applied the Bayesian mixing model presented in a groundwater context, it is generally applicable to a variety of mixing-related research questions, e.g., stream water mixing on a catchment scale. We hope that the available data set and source code will serve as a template for future studies to facilitate reliable estimates of groundwater mixing and ultimately improve water management.

Acknowledgments

All data and code used in this study can either be found in the Supplementary Information or are available online: <https://doi.org/10.25678/000183>. We thank Richard P. Hooper, two anonymous reviewers and the associate editor for their constructive comments and suggestions that helped to improve the manuscript. We also thank Benjamin Plüss, Reto Britt and Jonas Zbinden for their help in the field. Furthermore, we are grateful for technical support in the ETH Noble Gas laboratory provided by Henner Busemann and Colin Maden, and the assistance provided by Edith Horstmann and Alexandra Lightfoot. The AUA laboratory at Eawag is thanked for the analysis of the hydro-chemical data. A.L.P. gratefully acknowledges financial support for this work from the EU Framework Programme for Research and Innovation Horizon 2020 ITN “Hypotrain” (Marie Skłodowska-Curie grant agreement No. 641939) and Eawag.

References

- Abbott, B. W., Baranov, V., Mendoza-Lera, C., Nikolakopoulou, M., Harjung, A.,
Kolbe, T., ... Pinay, G. (2016). Using multi-tracer inference to move be-
yond single-catchment ecohydrology. *Earth-Science Rev.*, 160, 19–42. doi:
10.1016/j.earscirev.2016.06.014
- Arendt, C. A., Aciego, S. M., & Hetland, E. A. (2015). An open source Bayesian
Monte Carlo isotope mixing model with applications in Earth surface pro-
cesses. *Geochemistry, Geophys. Geosystems*, 16(5), 1274–1292. doi:
10.1002/2014GC005683
- Barthold, F. K., Tyralla, C., Schneider, K., Vaché, K. B., Frede, H. G., & Breuer,
L. (2011). How many tracers do we need for end member mixing analy-
sis (EMMA)? A sensitivity analysis. *Water Resour. Res.*, 47(8), 1–14. doi:
10.1029/2011WR010604
- Batlle-Aguilar, J., Banks, E. W., Batelaan, O., Kipfer, R., Brennwald, M. S., &
Cook, P. G. (2017). Groundwater residence time and aquifer recharge in multi-
layered, semi-confined and faulted aquifer systems using environmental tracers.
J. Hydrol., 546, 150–165. doi: 10.1016/j.jhydrol.2016.12.036
- Bernal, S., Butturini, A., & Sabater, F. (2006). Inferring nitrate sources through end
member mixing analysis in an intermittent Mediterranean stream. *Biogeochem-
istry*, 81(3), 269–289. doi: 10.1007/s10533-006-9041-7
- Beyerle, U., Aeschbach-Hertig, W., Hofer, M., Imboden, D. M., Baur, H., & Kipfer,
R. (1999). Infiltration of river water to a shallow aquifer investigated
with $^3\text{H}/^3\text{He}$, noble gases and CFCs. *J. Hydrol.*, 220(3-4), 169–185. doi:
10.1016/S0022-1694(99)00069-4
- Blake, W. H., Boeckx, P., Stock, B. C., Smith, H. G., Bodé, S., Upadhayay, H. R.,
... Semmens, B. X. (2018). A deconvolutional Bayesian mixing model ap-
proach for river basin sediment source apportionment. *Sci. Rep.*, 8(1), 13073.
doi: 10.1038/s41598-018-30905-9

- 580 Brennwald, M. S., Schmidt, M., Oser, J., & Kipfer, R. (2016). A Portable
581 and Autonomous Mass Spectrometric System for On-Site Environmen-
582 tal Gas Analysis. *Environ. Sci. Technol.*, 50(24), 13455–13463. doi:
583 10.1021/acs.est.6b03669
- 584 Brewer, M. J., Soulsby, C., & Dunn, S. M. (2002). A Bayesian Model for Composi-
585 tional Data Analysis. In W. Härdle & B. Rönz (Eds.), *Compstat* (p. 105-110).
586 Physica-Verlag HD.
- 587 Carpenter, B., Gelman, A., Hoffman, M., Lee, D., Goodrich, B., Betancourt, M., ...
588 Riddell, A. (2017). Stan: A probabilistic programming language. *Journal of*
589 *Statistical Software, Articles*, 76(1), 1–32. doi: 10.18637/jss.v076.i01
- 590 Carrera, J., Vázquez-Suñé, E., Castillo, O., & Sánchez-Vila, X. (2004). A method-
591 ology to compute mixing ratios with uncertain end-members. *Water Resour.*
592 *Res.*, 40(12), 1–11. doi: 10.1029/2003WR002263
- 593 Christophersen, N., & Hooper, R. P. (1992). Multivariate Analysis of Stream
594 Water Chemical Data: The Use of Principal Components Analysis for the
595 End-Member Mixing Problem. *Water Resour. Res.*, 28(1), 99–107.
- 596 Christophersen, N., Neal, C., Hooper, R. P., Vogt, R. D., & Andersen, S. (1990).
597 Modelling streamwater chemistry as a mixture of soilwater end-members—A
598 step towards second-generation acidification models. *J. Hydrol.*, 116(1-4),
599 307–320. doi: 10.1016/0022-1694(90)90130-P
- 600 Cook, P., & Dogramaci, S. (2019). Estimating Recharge from Recirculated Ground-
601 water with Dissolved Gases: An End-Member Mixing Analysis. *Water Resour.*
602 *Res.*. doi: 10.1029/2019WR025012
- 603 Cook, P., & Herczeg, A. L. (2000). *Environmental Tracers in Subsurface Hydrology*
604 (Vol. 53) (No. 9). Springer Science+Business Media New York. doi: 10.1017/
605 CBO9781107415324.004
- 606 Currell, M. J., & Cartwright, I. (2011). Major-ion chemistry, $\delta^{13}\text{C}$ and $^{87}\text{Sr}/^{86}\text{Sr}$
607 as indicators of hydrochemical evolution and sources of salinity in ground-

- 608 water in the Yuncheng Basin, China. *Hydrogeol. J.*, 19(4), 835–850. doi:
609 10.1007/s10040-011-0721-6
- 610 Davis, P., Syme, J., Heikoop, J., Fessenden-Rahn, J., Perkins, G., Newman, B.,
611 ... Hagerty, S. B. (2015). Quantifying uncertainty in stable isotope
612 mixing models. *J. Geophys. Res. Biogeosciences*, 120(5), 903–923. doi:
613 10.1002/2014JG002839
- 614 Delsman, J. R., Oude Essink, G. H., Beven, K. J., & Stuyfzand, P. J. (2013).
615 Uncertainty estimation of end-member mixing using generalized likelihood un-
616 certainty estimation (GLUE), applied in a lowland catchment. *Water Resour.*
617 *Res.*, 49(8), 4792–4806. doi: 10.1002/wrcr.20341
- 618 Dogramaci, S., Skrzypek, G., Dodson, W., & Grierson, P. F. (2012). Stable iso-
619 tope and hydrochemical evolution of groundwater in the semi-arid Hamersley
620 Basin of subtropical northwest Australia. *J. Hydrol.*, 475, 281–293. doi:
621 10.1016/j.jhydrol.2012.10.004
- 622 Erhardt, E. B., & Bedrick, E. J. (2013). A Bayesian framework for stable isotope
623 mixing models. *Environ. Ecol. Stat.*, 20(3), 377–397. doi: 10.1007/s10651-012
624 -0224-1
- 625 Gardner, W. P., Harrington, G. A., Solomon, D. K., & Cook, P. G. (2011). Us-
626 ing terrigenic ^4He to identify and quantify regional groundwater discharge to
627 streams. *Water Resour. Res.*, 47(6), 1–13. doi: 10.1029/2010WR010276
- 628 Hooper, R. P. (2003). Diagnostic tools for mixing models of stream water chemistry.
629 *Water Resour. Res.*, 39(3), 55–61. doi: 10.1029/2002WR001528
- 630 Hooper, R. P., Christophersen, N., & Peters, N. E. (1990). Modelling streamwa-
631 ter chemistry as a mixture of soilwater end-members—An application to the
632 Panola Mountain catchment, Georgia, U.S.A. *J. Hydrol.*, 116(1-4), 321–343.
633 doi: 10.1016/0022-1694(90)90131-G
- 634 Jasechko, S. (2016). Partitioning young and old groundwater with geochemical trac-
635 ers. *Chem. Geol.*, 427, 35–42. doi: 10.1016/j.chemgeo.2016.02.012

- Kavetski, D., Kuczera, G., & Franks, S. W. (2006). Bayesian analysis of input uncertainty in hydrological modeling: 1. theory. *Water Resour. Res.*, *42*(3).
- Kruschke, J. K. (2015). Markov Chain Monte Carlo. In *Doing Bayesian Data Analysis* (2nd ed., pp. 143–191). Academic Press. doi: 10.1016/B978-0-12-405888-0.00007-6
- Kulongoski, J. T., Hilton, D. R., Cresswell, R. G., Hostetler, S., & Jacobson, G. (2008). Helium-4 characteristics of groundwaters from Central Australia: Comparative chronology with chlorine-36 and carbon-14 dating techniques. *J. Hydrol.*, *348*(1-2), 176–194. doi: 10.1016/j.jhydrol.2007.09.048
- Marty, B., Torgersen, T., Meynier, V., O’Nions, R. K., & de Marsily, G. (1993). Helium isotope fluxes and groundwater ages in the Dogger Aquifer, Paris Basin. *Water Resour. Res.*, *29*(4), 1025–1035. doi: 10.1029/93WR00007
- Moeck, C., Affolter, A., Radny, D., Dressmann, H., Auckenthaler, A., Huggenberger, P., & Schirmer, M. (2017). Improved water resource management for a highly complex environment using three-dimensional groundwater modelling. *Hydrogeol. J.* doi: 10.1007/s10040-017-1640-y
- Moeck, C., Molson, J., & Schirmer, M. (2019). Pathline density distributions in a Null-Space Monte Carlo approach to assess groundwater pathways. *Groundwater*. doi: 10.1111/gwat.12900
- Moeck, C., Radny, D., Auckenthaler, A., Berg, M., Hollender, J., & Schirmer, M. (2017). Estimating the spatial distribution of artificial groundwater recharge using multiple tracers. *Isotopes Environ. Health Stud.*, *53*(5), 484–499. doi: 10.1080/10256016.2017.1334651
- Moeck, C., Radny, D., Borer, P., Rothardt, J., Auckenthaler, A., Berg, M., & Schirmer, M. (2016). Multicomponent statistical analysis to identify flow and transport processes in a highly-complex environment. *J. Hydrol.*, *542*, 437–449. doi: 10.1016/j.jhydrol.2016.09.023
- Moeck, C., Radny, D., Popp, A., Brennwald, M., Stoll, S., Auckenthaler, A., ...

- Schirmer, M. (2017). Science of the Total Environment Characterization of a managed aquifer recharge system using multiple tracers. *Sci. Total Environ.*, *609*, 701–714. doi: 10.1016/j.scitotenv.2017.07.211
- Müller, T., Osenbrück, K., Strauch, G., Pavetich, S., Al-Mashaikhi, K. S., Herb, C., ... Sanford, W. (2016). Use of multiple age tracers to estimate groundwater residence times and long-term recharge rates in arid southern Oman. *Appl. Geochemistry*, *74*, 67–83. doi: 10.1016/j.apgeochem.2016.08.012
- Parnell, A., & Inger, R. (2019). *Stable Isotope Mixing Models in R with simmr* (Tech. Rep.). Retrieved from <https://cran.r-project.org/web/packages/simmr/vignettes/simmr.html>
- Pelizardi, F., Bea, S. A., Carrera, J., & Vives, L. (2017). Identifying geochemical processes using End Member Mixing Analysis to decouple chemical components for mixing ratio calculations. *J. Hydrol.*, *550*, 144–156. doi: 10.1016/j.jhydrol.2017.04.010
- Piper, A. M. (1944). A graphic procedure in the geochemical interpretation of water-analyses. *Trans. Am. Geophys. Union*, *25*(6), 914. doi: 10.1029/TR025i006p00914
- Price, M., Swart, P. K., & Price, R. M. (2003). Use of tritium and helium to define groundwater flow conditions in Everglades National Park. *Water Resour. Res.*, *39*(9), 1–12. doi: 10.1029/2002WR001929
- R Core Team. (2018). R: A language and environment for statistical computing [Computer software manual]. Vienna, Austria.
- Rueedi, J., Purtschert, R., Beyerle, U., Alberich, C., & Kipfer, R. (2005). Estimating groundwater mixing ratios and their uncertainties using a statistical multi parameter approach. *J. Hydrol.*, *305*, 1–14. doi: 10.1016/j.jhydrol.2004.06.044
- Sanborn, M. E., Souders, A. K., Wimpenny, J., Yin, Q.-Z., & Young, M. (2016). Bayesian nitrate source apportionment to individual groundwater wells in the Central Valley by use of elemental and isotopic tracers. *Water Resour. Res.*,

- 692 1–21. doi: 10.1002/2015WR018523
- 693 Skrzypek, G., Dogramaci, S., & Grierson, P. F. (2013). Geochemical and hy-
 694 drological processes controlling groundwater salinity of a large inland wet-
 695 land of northwest Australia. *Chem. Geol.*, *357*, 164–177. doi: 10.1016/
 696 j.chemgeo.2013.08.035
- 697 Soulsby, C., Petry, J., Brewer, M., Dunn, S., Ott, B., & Malcolm, I. (2003). Identi-
 698 fying and assessing uncertainty in hydrological pathways: a novel approach to
 699 end member mixing in a Scottish agricultural catchment. *J. Hydrol.*, *274*(1-4),
 700 109–128. doi: 10.1016/S0022-1694(02)00398-0
- 701 Spottke, I., Zechner, E., & Huggenberger, P. (2005). The southeastern border
 702 of the Upper Rhine Graben: A 3D geological model and its importance for
 703 tectonics and groundwater flow. *Int. J. Earth Sci.*, *94*(4), 580–593. doi:
 704 10.1007/s00531-005-0501-4
- 705 Stute, M., Sonntag, C., Deák, J., & Schlosser, P. (1992). Helium in deep circulating
 706 groundwater in the Great Hungarian Plain: Flow dynamics and crustal and
 707 mantle helium fluxes. *Geochim. Cosmochim. Acta*, *56*(5), 2051–2067. doi:
 708 10.1016/0016-7037(92)90329-H
- 709 Tetzlaff, D., Buttle, J., Carey, S. K., McGuire, K., Laudon, H., & Soulsby, C.
 710 (2015). Tracer-based assessment of flow paths, storage and runoff genera-
 711 tion in northern catchments: a review. *Hydrol. Process.*, *29*(16), 3475–3490.
 712 doi: 10.1002/hyp.10412
- 713 Turnadge, C., & Smerdon, B. D. (2014). A review of methods for modelling environ-
 714 mental tracers in groundwater: Advantages of tracer concentration simulation.
 715 *J. Hydrol.*, *519*, 3674–3689. doi: 10.1016/j.jhydrol.2014.10.056
- 716 Valder, J. F., Long, A. J., Davis, A. D., & Kenner, S. J. (2012). Multivariate sta-
 717 tistical approach to estimate mixing proportions for unknown end members. *J.*
 718 *Hydrol.*, *460-461*, 65–76. doi: 10.1016/j.jhydrol.2012.06.037